EXPERIMENTAL RESULTS ON EXCLUSIVE VECTOR MESONS AND HEAVY QUARKONIUM

P. THOMPSON

This contribution reviews recent experimental results on the production of light and heavy vector mesons from the H1 and ZEUS collaborations during HERA-I data taking. The data are compared in detail with the predictions of theoretical models based on perturbative QCD.

1. Introduction

The study of vector meson production at HERA provides an experimentally clean process which allows the nature of the strong interaction at high energy to be investigated. HERA is a unique facility which allows simultaneous control of the different kinematic scales: the squared mass of the vector meson, $M^2_{\rm VM}$, the virtuality of the exchanged photon, Q^2, and the four-momentum transferred at the proton vertex, t. The studies at HERA involve identifying transitions from long range, or soft, to short distance, or hard, behaviour as a function of the various scales, in order to test the applicability of perturbative QCD (pQCD). It is hoped the study of hard diffraction processes will lead to a better understanding of the vacuum-exchange and the strong interaction.

The kinematics for exclusive, or diffractive, vector meson production $ep \rightarrow e({\rm VM})Y$ are described in terms of the ep centre-of-mass-energy squared $s = (k + p)^2$, the virtuality of the photon $Q^2 = -q^2 = -(k - k')^2$, the square of the centre-of-mass energy of the initial photon-proton system $W^2 = (q + p)^2$ and the four-momentum transfer squared $t = (p - p_Y)^2$. Here k (k') is the four-momentum of the incident (scattered) lepton and q is the four-momentum of the virtual photon. The four-momentum of the incident proton is denoted by p and p_Y is the four-momentum of the system Y, which represents either an elastically scattered proton or a dissociated proton system.

2. Vector Meson Dominance and Regge Theory

In the Vector Meson Dominance (VMD) model the photon is assumed to fluctuate into a vector meson at a large distance before the target with the vector meson subsequently undergoing a soft scattering from the proton target. In the model, the vector meson retains the helicity of the photon and, therefore, s-channel helicity conservation (SCHC) is satisfied. The VMD model can be combined with Regge phenomenology, which has been successful in parameterising soft hadronic elastic and total cross sections. At high energy, in Regge theory, the cross section is dominated by the "soft pomeron" trajectory with an intercept $\alpha_{I\!P}(0) = 1.08$ and a slope $\alpha'_{I\!P}(t) = 0.25$ GeV^2 [1]. The intercept describes the experimentally observed weak energy dependence $\sim W^{0.2}$ of the total and elastic hadron-hadron cross sections using $\sigma_{tot} \propto W^{\delta}$ where $\delta = 2(\alpha_{I\!P}(0) - 1)$. The soft pomeron is characterised by scattering at small angles and exhibits an exponential t dependence $d\sigma/dt \propto e^{b(W)t}$, where $b(W)$ is the slope parameter. The foward scattering shows a logarithmic shrinkage with increasing W given by $b = b_0 + 4\alpha'_{I\!P} \log(W/W_0)$.

3. The Dipole Picture and QCD

An increasingly popular approach to describe diffractive interactions is to consider the scattering of $q\bar{q}$ fluctuations of the virtual photon, as colour dipoles scattering off the proton target in the proton rest frame. The probability of the photon to fluctuate into a $q\bar{q}$ pair may be parameterised in QCD using the vector meson wave function. The interaction of the dipole with the proton is described at lowest order by the exchange of two gluons in a colour singlet state. In the leading logarithmic (LL) approximation, this process is described by the effective exchange of a gluonic ladder and the cross section is related to the gluon density within the proton. In QCD, the transverse separation of the dipole is given by $r \sim \frac{1}{(z(1-z)Q^2+m_q^2)^{1/2}}$, where m_q is the mass of the quark and z is the longitudinal momentum fraction of the photon carried by the quark. Therefore, at large Q^2 or large m_q^2 the dipole may resolve short distances within the proton suggesting that perturbative QCD may be applicable. In contrast, at small Q^2 and small m_q^2 the dipole will be large and the process is likely to contain a significant non-perturbative component.

There are many different approaches combining the dipole approach and pQCD [2,3,4,5,6]. However, the majority of the models have common features, and include the following. A fast rise of the cross section with W

($\sigma \sim W^{0.8}$) due to the rise of the proton gluon density at low x. At asymptotically large Q^2, the cross section for longitudinally polarised photons is expected to dominate. The Q^2 dependence in the longitudinally polarised cross section is expected to be slower than $1/Q^6$ due to the effect of the gluon density. The transverse cross section is expected to have a $1/Q^8$ dependence, although endpoint effects in the wavefunctions of light vector mesons mean that there may be large non-perturbative contributions. At low $|t|$, the $|t|$-dependence is expected to be universal and the two gluon form-factor leads to $\mathrm{d}\sigma/\mathrm{d}t \propto e^{-4|t|}$, with little or no shrinkage expected.

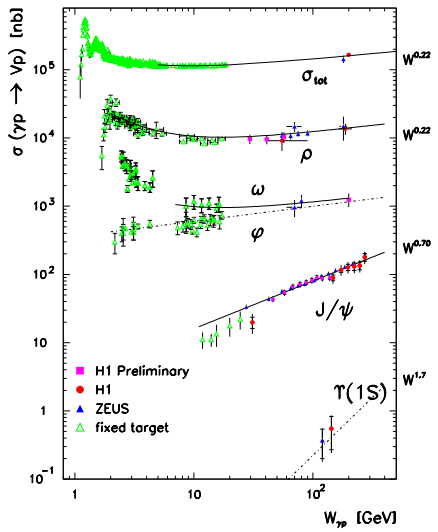

Figure 1. The cross section versus W of the elastic photoproduction of ρ, ω, ϕ, J/ψ and Υ vector mesons.

4. Elastic Vector Meson Photoproduction and Energy Dependence

In figure 1 the cross section for vector meson photoproduction is shown as a function of the centre-of-mass energy W, integrated over low values of $|t|$. The light vector mesons show an energy dependence compatible with the soft pomeron, whereas the J/ψ shows a steeper behaviour $\sim W^{0.7}$. The J/ψ energy dependence is qualitatively described by pQCD models [4,5] which use the mass of the J/ψ as a perturbative scale. The J/ψ data may be used to

study the W dependence at different values of t, in order to measure the pomeron trajectory for the process. The intercept and the slope are found to be $\alpha_{I\!P}(0) \sim 1.2$ and $\alpha'_{I\!P} \sim 0.1$ GeV^2 [7,8], respectively, incompatible with the trajectory of the soft pomeron derived from hadron-hadron scattering.

5. Energy Dependence in Elastic Electroproduction

The variation of the energy dependence with Q^2 has been studied with increasing accuracy for the ρ meson [9,10]. The W dependence is found to become steeper with increasing Q^2 and tends toward the same value as J/ψ photoproduction, indicating that Q^2 is a possible scale for the hard process. As yet, there are no quantitative models to which the data can be compared. The variation of the W dependence with Q^2 has also been studied in J/ψ production [11]. The energy dependence is found to be similar at all values of Q^2. The J/ψ data are qualitatively described by pQCD models in which the steep energy dependence arises from the gluon density of the proton [4,6]. The pomeron trajectory for J/ψ production was measured with increasing precision at $\langle Q^2 \rangle = 6.8$ GeV^2, and is found to be compatible with that measured in photoproduction.

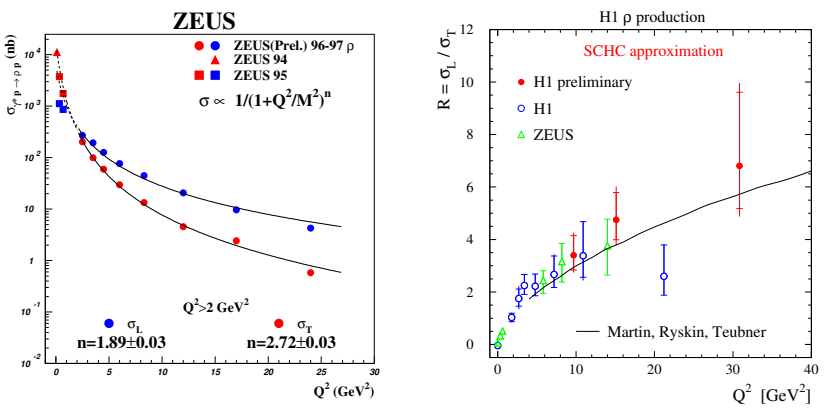

Figure 2. (left) The cross sections σ_L and σ_T and (right) the ratio $R = \sigma_L/\sigma_T$ as a function of Q^2 for elastic ρ electroproduction

6. Q^2 Dependence in Elastic Electroproduction

In pQCD, the cross sections for longitudinally and transversely polarised photons are expected to have different Q^2 dependences. The Q^2 dependence of the two components has been studied in ρ production [9,10]. In figure 2, the data are parameterised according to $1/(1+Q^2/M^2)^n$. For the longitudinal cross section a value of $n = 1.89 \pm 0.03$ is found which is consistent with the prediction of pQCD. The parameterisation is found to be inadequate for $Q^2 < 5$ GeV^2, which is thought to be attributable to wave function effects. The ratio $R = \sigma_L/\sigma_T$ is also shown in the figure. The increase of the ratio with Q^2 is compatible with calculations [4] based on wave particle duality using the details of the wavefunction. The Q^2 dependence of the cross section in J/ψ production has also been studied [11], although the determination of R, which is obtained from helicity frame measurements, is not possible due to limited statistics. The functional form $(Q^2+M^2)^{-n}$ is found to fit the J/ψ data, although the χ^2 of the fit improves considerably as the minimum Q^2 of the fit is increased. Models based on pQCD are able to give a reasonable description of the J/ψ data.

7. t-dependence at low t

The t-dependence at low $|t|$ is found to be well described by an exponential form $\sim e^{bt}$. The b-slope of the ρ decreases with increasing Q^2, whereas the J/ψ b-slope is constant with Q^2. At large Q^2 or large $M^2_{\rm VM}$ the b-slope has the value $b \sim 4.5$ GeV^2, suggestive of an underlying t-dependence which is a feature of pQCD models.

8. Helicity Measurements

The measurement of helicity angles gives information on the spin density matrix elements [12], which in turn are related to the helicity transition amplitudes. Precise measurements for ρ and ϕ elecroproduction [13] have established small violations of SCHC in r^5_{00} indicating that the dominant single helicity flip amplitude is T_{01}. The data are well described by a pQCD model [14] based on two gluon exchange in which the SCHC violation is attainable if the longitudinal momentum of the photon is shared asymmetrically by the $q\bar{q}$ pair. The measurements have been extended [15] as a function of $|t|$ in events where the final state proton dissociates into a low mass state. In figure 3, combinations of spin-density matrix elements show increasing SCHC violations with increasing $|t|$, which are well described

by the pQCD model. The spin density matrix element dependent on R ($R = \sigma_L/\sigma_T$) is observed to be constant in the t range studied, indicating that the b-slopes for σ_L and σ_T in ρ proton dissociation are similar. This is suggestive that the non-perturbative contribution to σ_T is small. This is further supported by the measurement of elastic ρ electroproduction [9] in which R was found to be constant as a function of W.

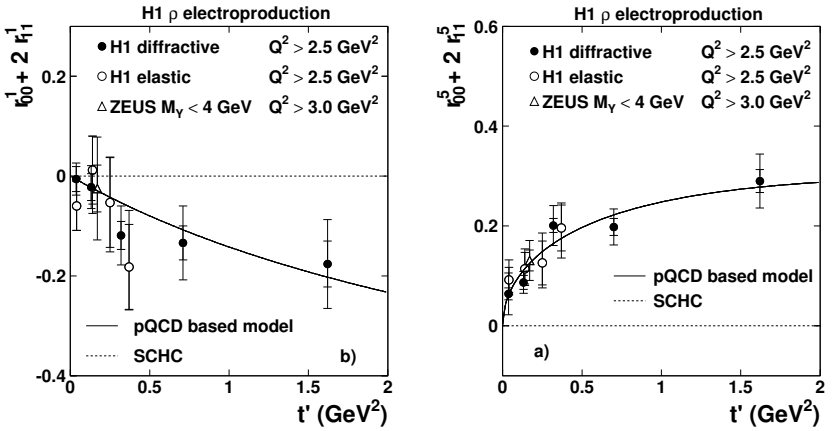

Figure 3. Measurements of (left) $r^5_{00} + 2r^5_{11}$ and (right) $r^1_{00} + 2r^1_{11}$ as a function of t.

9. Vector Meson Production at Large t

The diffractive photoproduction of vector mesons with large negative momentum transfer squared t at the proton vertex is a powerful means to probe the parton dynamics of the diffractive exchange. The variable t provides a relevant scale to investigate the application of pQCD. At sufficiently low values of Bjorken x (i.e. large values of the centre-of-mass energy W), the gluon ladder is expected to include contributions from BFKL evolution [16], as well as from standard DGLAP evolution [17].

Perturbative QCD models for the photoproduction of $J\psi$ mesons have been developed in the leading logarithmic approximation using either BFKL [18,19,20,21] or DGLAP [22] evolution. In the pQCD models, a non-relativistic approximation [23] for the J/ψ wavefunction is used in which the longitudinal momentum of the vector meson is shared equally between the quark and the anti-quark. In this approximation, the vector meson retains

the helicity of the photon such that s-channel helicity conservation (SCHC) is satisfied [24].

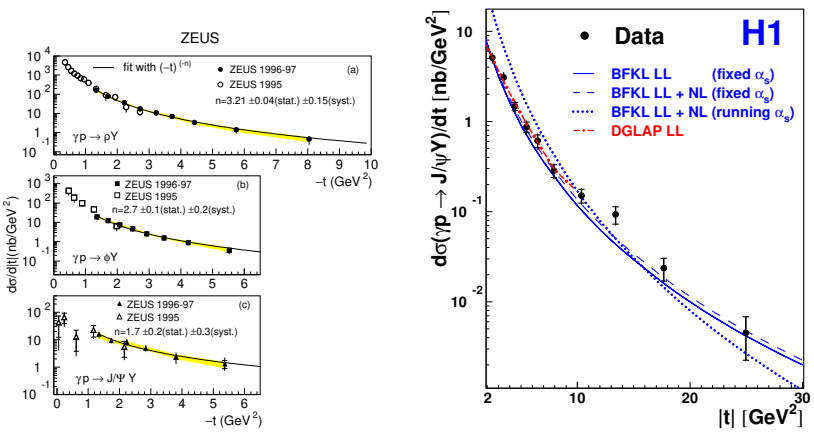

Figure 4. The cross section $d\sigma/dt$ for (left) ρ, ϕ and J/ψ photoproduction and (right) J/ψ photoproduction.

In figure 4, the large $|t|$ cross sections for ρ, ϕ and J/ψ [25,26] are shown. The data are described with a power law $\mathrm{d}\sigma/\mathrm{d}t \propto |t|^{-n}$, although the value of n in each case increases with the starting value of $|t|$ used in the fit. In figure 4 (right) the data are compared with the predictions from pQCD calculations in the BFKL leading logarithmic approximation [21] (solid curve), including non-leading corrections with fixed α_s [21] (dashed curve) and including non-leading corrections with running α_s [21] (dotted curve). The t dependence and normalisation of the data are well described by the BFKL LL approximation. The inclusion of NL corrections with a fixed strong coupling α_s leads to only a small difference with respect to the LL prediction. However, with a running α_s the t dependence becomes steeper and the prediction is unable to describe the data across the whole t range. The data are also well described by calculations in the DGLAP LL approximation [22] (dashed-dotted curve) in the region of validity for the model $|t| < M^2_{J/\psi}$.

In figure 5, the cross section is plotted as a function of W for different intervals of t, and also as a function of t in two different W regions. As can be seen from the plots, the W dependence is constant with t, and, the t dependence is constant with W. The LL BFKL model predicts a

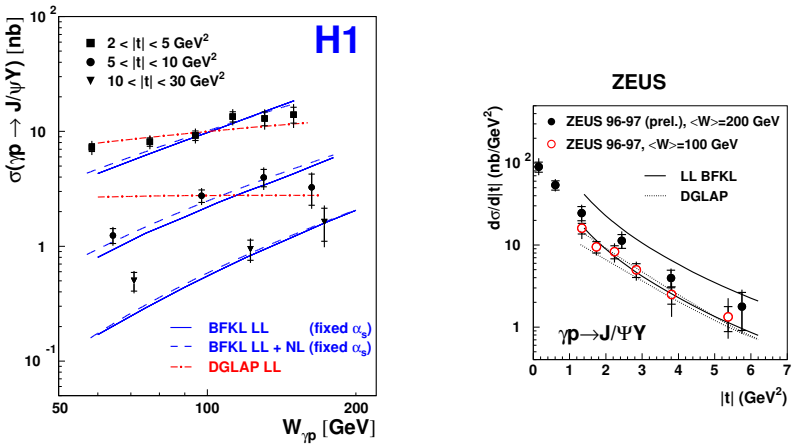

Figure 5. The cross section for J/ψ photoproduction (left) as a function of W in t-intervals (right) as a function of t at two different values of W.

stronger rise with W than is observed in the data, whereas the LL DGLAP model gives a flatter W dependence than the data. The cross section in W may be used to extract the pomeron trajectory assuming a linear form $\alpha_{I\!P}(t) = \alpha_{I\!P}(0) + \alpha'_{I\!P} t$, a fit to the three $\alpha_{I\!P}$ values yields a slope of $\alpha'_{I\!P} = -0.0135 \pm 0.0074\,(\text{stat.}) \pm 0.0051\,(\text{syst.})\ \text{GeV}^{-2}$ with an intercept of $\alpha_{I\!P}(0) = 1.167 \pm 0.048\,(\text{stat.}) \pm 0.024(\text{syst.})$. The value of the slope parameter α' is lower than that observed for the elastic photoproduction of J/ψ mesons at low $|t|$ [7]. It is also significantly different from the observations at low $|t|$ in hadron-hadron scattering.

To obtain information about the helicity structure of the interaction, the spin density matrix elements are extracted and shown in figure 6 as a function of $|t|$. In contrast to the ρ^0 meson, the measured spin density matrix elements of the J/ψ meson are all compatible with zero, within experimental errors, and are thus compatible with SCHC. The J/ψ results are therefore consistent with the longitudinal momentum of the photon being shared symmetrically between the heavy quarks. Hence, the approximations made in the pQCD models [18,19,20,22,21] for the J/ψ wavefunction are satisfactory for the present data.

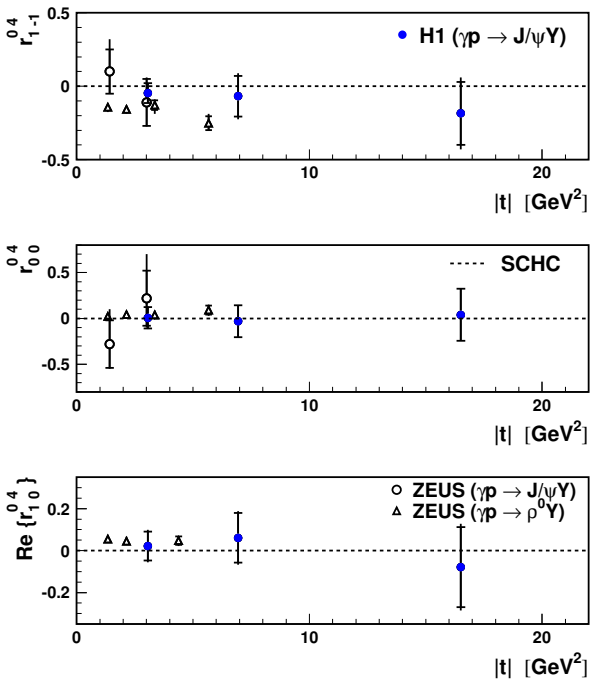

Figure 6. The three spin density matrix elements (top) r^{04}_{1-1}, (middle) r^{04}_{00} and (bottom) Re$\{r^{04}_{10}\}$ for the J/ψ as a function of $|t|$. The dashed line shows the expectation from SCHC. The results for the photoproduction of J/ψ and ρ^0 mesons [25] are also shown.

10. Summary

The exclusive production of vector mesons at HERA allows the dynamics of vacuum-exchange processes to be studied. The transition from soft to hard behaviour is observed with increasing Q^2 or $M^2_{\rm VM}$. The analysis of helicity structure provides unique insight into the structure of the vector meson wavefunctions. The production of vector mesons at high $|t|$ shows a hard behaviour in $|t|$ and W suggesting that processes beyond DGLAP may be necessary to describe the data. In general, pQCD has been able to provide qualitative descriptions of the experimental data and the second phase of HERA running will continue to improve our understanding of the strong interaction.

References

1. A. Donnachie and P. V. Landshoff, Nucl. Phys. B **231** (1984) 189.
2. S. J. Brodsky et al, Phys. Rev **50** (1994) 3134 [hep-ex/9402283].
3. J. C. Collins, L. Frankfurt and M. Strikman, Phys. Rev **56** (1997) 2982.
4. A. D. Martin, M. G. Ryskin and T. Teubner, Phys. Rev **55** (1997) 4329.
5. J. C. Collins, L. Frankfurt M. McDermott and M. Strikman, JHEP **103** (2001) 45.
6. L. Frankfurt W. Koepf and M. Strikman, Phys. Rev D **57** (1998) 512.
7. S. Chekanov *et al.* [ZEUS Collaboration], Eur. Phys. J. C **24** (2002) 345.
8. H1 Collaboration, abstract 108, paper to EPS Conference 2003, Aachen.
9. ZEUS Collaboration, abstract 594, paper to EPS Conference 2001, Budapest.
10. H1 Collaboration, abstract 092, paper to EPS Conference 2003, Aachen.
11. ZEUS Collaboration, abstract 813, paper to ICHEP Conference 2002, Amsterdam.
12. K. Schilling and G. Wolf, Nucl. Phys. B **61** (1973) 381.
13. H1 Collab., C. Adloff et al., Eur.Phys.J. C13 (2000) 371;
    H1 Collab., C. Adloff et al., Phys. Lett. B483 (2000) 360.
14. D.Yu. Ivanov, R. Kirshner, Phys. Rev **D58** (1998) 114026 [hep-ph/9907324].
15. H1 Collab., C. Adloff et al., Phys. Lett. B539 (2002) 25.
16. E. A. Kuraev, L. N. Lipatov and V. S. Fadin, Sov. Phys. JETP **44** (1976) 443 [Zh. Eksp. Teor. Fiz. **71** (1976) 840];
    I. I. Balitsky and L. N. Lipatov, Sov. J. Nucl. Phys. **28** (1978) 822 [Yad. Fiz. **28** (1978) 1597].
17. V. N. Gribov and L. N. Lipatov, Yad. Fiz. **15** (1972) 781 and 1218 [Sov. J. Nucl. Phys. **15** (1972) 438 and 675];
    G. Altarelli and G. Parisi, Nucl. Phys. B **126** (1977) 298.
18. J. R. Forshaw and M. G. Ryskin, Z. Phys. C **68** (1995) 137.
19. J. Bartels, J. R. Forshaw, H. Lotter and M. Wüsthoff, Phys. Lett. B **375** (1996) 301.
20. J. R. Forshaw and G. Poludniowski, Eur. Phys. J. C **26** (2003) 411.
21. R. Enberg, L. Motyka and G. Poludniowski, Eur. Phys. J. C **26** (2002) 219.
22. E. Gotsman, E. Levin, U. Maor and E. Naftali, Phys. Lett. B **532** (2002) 37.
23. M. G. Ryskin, Z. Phys. C **57** (1993) 89.
24. E. V. Kuraev, N. N. Nikolaev and B. G. Zakharov, JETP Lett. **68** (1998) 696 [Pisma Zh. Eksp. Teor. Fiz. **68** (1998) 667].
25. S. Chekanov *et al.* [ZEUS Collaboration], ons at large momentum transfer at HERA," Eur. Phys. J. C **26** (2003) 389.
26. H1 Collab., A. Aktas et al., Phys. Lett. B **568** (2003) 205.